Society For Biomaterials

Self-aggregation of amphiphilic [60]fullerenyl focal point functionalized PAMAM dendrons into pseudodendrimers: DNA binding involving dendriplex formation

Cheng-Hsiang Hung,[1] Wen-Wei Chang,[2] Ssu-Ching Liu,[2] Shang-Jung Wu,[1] Chih-Chien Chu,[1,3] Ya-Ju Tsai,[4] Toyoko Imae[4]

[1]School of Medical Applied Chemistry, Chung Shan Medical University, Taichung 40201, Taiwan
[2]School of Biomedical Sciences, Chung Shan Medical University, Taichung 40201, Taiwan
[3]Department of Medical Education, Chung Shan Medical University Hospital, Taichung 40201, Taiwan
[4]Graduate Institute of Applied Science and Technology, National Taiwan University of Science and Technology, Taipei 10607, Taiwan

Received 8 May 2014; revised 22 July 2014; accepted 23 July 2014
Published online 11 August 2014 in Wiley Online Library (wileyonlinelibrary.com). DOI: 10.1002/jbm.a.35299

Abstract: In this research, we successfully performed a "click" synthesis of amphiphilic poly(amido amine) dendron-bearing fullerenyl conjugate ($C_{60}G_1$) using a copper(I)-catalyzed azide-alkyne cycloaddition reaction. The strong hydrophobicity of the C_{60} moiety induces self-assembly of $C_{60}G_1$ into core–shell-like "pseudodendrimers" with a uniform size distribution and positively charged peripherals. The pseudodendrimers were well-characterized by atomic force microscopy (AFM), transmission electron microscopy, and dynamic light scattering. On the basis of electrostatic interactions, the polycationic $C_{60}G_1$ assembly can serve as a nonviral gene vector. An ethidium bromide displacement assay and agarose gel electrophoresis both indicated that $C_{60}G_1$ assembly forms stable complexes with the cyclic reporter gene (pEGFP-C1) at low nitrogen-to-phosphorous (N/P) ratios. AFM analysis revealed a dynamic complex-formation process, and confirmed the synthesis of $C_{60}G_1$/pEGFP-C1 hybrids with a particle dimensions less than 200 nm. Fluorescence microscopy and flow cytometry revealed that 51% of HeLa and 43% of MCF-7 cells are positive to the YOYO-1-labeled hybrids at an N/P ratio of 2, being comparable to TurboFect-mediated delivery. © 2014 Wiley Periodicals, Inc. J Biomed Mater Res Part A: 103A: 1595–1604, 2015.

Key Words: amphiphilic dendrons, fullerene, gene delivery, PAMAM dendrimer, click chemistry

How to cite this article: Hung C-H, Chang W-W, Liu S-C, Wu S-J, Chu C-C, Tsai Y-J, Imae T. 2015. Self-aggregation of amphiphilic [60]fullerenyl focal point functionalized PAMAM dendrons into pseudodendrimers: DNA binding involving dendriplex formation. J Biomed Mater Res Part A 2015:103A:1595–1604.

INTRODUCTION

Poly(amido amine) (PAMAM) dendrimers are considered to be biocompatible, nonimmunogenic drug and gene vehicles because they demonstrate remarkable effectiveness for *in vitro* and *in vivo* medication delivery.[1–5] However, PAMAM toxicity profiles are problematic for biomedical applications because of the presence of polycationic substituents, and their persistence in cells. Alternatively, using the dendron architectures in which a hydrophobic group at the focal point encourages self-assembly of the resulting amphiphilic dendrons into large "pseudodendrimers."[6,7] This supramolecular strategy is a novel concept in the field of dendrimer-mediated nucleic acid delivery.[8–14] In addition, this type of dendrimers combing the characteristics of cationic polymers and lipids, can give rise to synergistic effects in gene delivery.

Carbon-based nanomaterials, such as fullerenes, nanotubes, and graphene have attracted considerable interest for their biomedical applications, because of their unique *in vitro* and *in vivo* biodistributions and functionalities.[15–18] In particular, fullerene derivatives that combine 3-dimensionality with defined physiochemical properties are promising candidates for the preparation of bioactive molecules with unique biodistributions.[19] Nakamura and coworkers[20–23] pioneered stable DNA-C_{60} hybrids that are capable of effective cell transfection, not only of mammalian cells, but also of pregnant female ICR mice, with distinct organ selectivity; they conducted a systematic structure–activity relationship investigation on a library of 22 cationic fullerene derivatives, and proposed that an appropriate hydrophilic–lipophilic balance (HLB) is essential to synthesize DNA–fullerene complexes for effective gene transfection.

Additional Supporting Information may be found in the online version of this article.
Correspondence to: C.-C. Chu; e-mail: jrchu@csmu.edu.tw
Contract grant sponsor: Chung Shan Medical University and the National Science Council of Taiwan, Republic of China; contract grant number: NSC100-2113-M-040-007-MY2

Although variations in transfection protocol and cell type can dramatically affect transfection efficiency, the size, and morphology of the DNA–vector complexes are also critical parameters to accomplish efficient gene delivery. Pristine C_{60} is an extremely solvophobic and water-insoluble molecule, and thus the presence of hydrophilic pendant groups confer greater solubility in aqueous media, essential for biological applications.[24–26] However, the amphiphilic nature of such water-soluble C_{60} derivatives usually results in spontaneous self-aggregation in aqueous media. Thus, careful manipulation of the amphiphilic counterpart is necessary to achieve a more favorable HLB to form stable gene vehicles with appropriate shape and morphology (e.g., spheroid or vesicle-like), thus facilitating DNA complexation, cellular uptake, and gene transfection.[27–30]

In the current study, we demonstrate a facile synthesis of amphiphilic PAMAM dendron-bearing fullerene derivative, by using an efficient Cu(I)-catalyzed azide-alkyne cycloaddition (CuAAC).[31] We found that the click cluster, interconnecting the diazido-functionalized fullerene and PAMAM dendrons bearing a propargyl focal point via a 1,4-triazole linkage, is highly water-soluble and is readily prepared in high yield without the need for chromatographic purification. Amphiphilic dendrons containing an extremely hydrophobic fullerene moiety and a hydrophilic PAMAM dendritic scaffold, favor the formation of nanoparticles with a uniform size distribution in water. Atomic force microscopy (AFM) analysis revealed that these particles could condense plasmid DNA into stable complexes with desirable dimensions, at low nitrogen-to-phosphorus (N/P) ratios. Moreover, the fullerodendron assembly also exhibited remarkable gene delivery efficiency toward the target cell lines.

EXPERIMENT

Materials and instruments

Pure C_{60} was purchased from Uni-onward Corporation and used as received. Other chemicals used for organic synthesis were obtained as high-purity reagent-grade chemicals from either Acros or Sigma-Aldrich and used without further purification. Organic solvents were AR grade and purchased from either Mallinckrodt or Echo chemicals. Ethylenediamine (EDA) and dichloromethane (DCM) were dried over calcium hydride under N_2 before used. Tetrahydrofuran (THF) and toluene were distilled over sodium under N_2 in the presence of benzophenone as the indicator prior to use.

Gel permeation chromatography (GPC) was conducted at 35°C using a Shodex Sugar KS-802 column on an assembled instrument that was equipped with pump (Water Model-501), column oven, and refractive index detector (Schambeck SFD GmbH, RI-2000) connected in series. ^{1}H (400 MHz)- and ^{13}C (100 MHz)-NMR spectra were recorded on a Varian Mercury Plus 400 MHz spectrometer at room temperature using $CDCl_3$, DMSO-d_6, or D_2O as the solvent. Spectral processing (Fourier transform, peak assignment and integration) was performed using MestReNova 6.2.1 software. Matrix-assisted laser desorption ionization/time-of-flight mass spectrometry (MALDI-TOF-MS) was performed on a Bruker AutoFlex III TOF/TOF system in positive ion mode using either 2,5-dihydroxybenzoic acid or α-cyano-4-hydroxycinnamic acid as the desorption matrix. Fourier-transform infrared (FT-IR) and ultraviolet–visible (UV–Vis) absorption spectra were performed on a Bruker Alpha FT spectrometer and on a Thermo Genesys 10S UV–Vis spectrometer, respectively. Fluorescence spectroscopic analysis was carried out either on a Hitachi F-2500 spectrometer or on a Molecular Devices FlexStation 3 microplate reader at 25°C.

Synthesis of PAMAM dendron G_1

A methanol solution (370 mL) of propargylamine (6.01 g, 0.109 mol) was added slowly into a methanol solution (110 mL) of methyl acrylate (28.1 g, 0.326 mol) under 0°C. The reaction mixture was allowed to warm to room temperature and stirred for 3 days. The volatiles were removed under reduced pressure using a rotary evaporation to give half-generation dendron quantitatively. Then this compound (6.25 g, 27.5 mmol) dissolved in dry methanol (90 mL) was added dropwise into a methanol solution (370 mL) of EDA (66.1 g, 1.1 mol) under 0°C over a period of 30 min. The reaction mixture was allowed to warm to room temperature and stirred for 3 days under a N_2 balloon until complete disappearance of terminal methyl ester groups. The solvent was removed under reduced pressure using a rotary evaporation, and excess EDA was carefully removed by azeotropic distillation at 35°C using toluene and methanol mixture (9:1) to afford product **G_1** as a yellowish gum (30.0 g, 97%). ^{1}H-NMR (400 MHz, $CDCl_3$): $\delta = 2.22$ (t, $J = 2.3$ Hz, 1H), 2.38 (t, $J = 5.8$ Hz, 4H), 2.81–2.86 (m, 8H), 3.29 (dd, $J = 11.6$, 5.8 Hz, 4H), and 3.43 (d, $J = 2.3$ Hz, 2H).

Synthesis of PAMAM dendron G_2

A methanol solution (40 mL) of **G_1** (3.44 g, 12.1 mmol) was added slowly into a methanol solution (25 mL) of methyl acrylate (6.27 g, 72.8 mmol) under 0°C. The reaction mixture was allowed to warm to room temperature and stirred for 3 days. The volatiles were removed under reduced pressure using a rotary evaporation to give half-generation dendron quantitatively. This compound (6.39 g, 10.2 mmol) dissolved in dry methanol (35 mL) was added dropwise to a methanol solution (270 mL) of EDA (48.9 g, 0.814 mol) under 0°C over a period of 30 min. The reaction mixture was allowed to warm to room temperature and stirred for 3 days under a N_2 balloon until complete disappearance of terminal methyl ester groups. The solvent was removed under reduced pressure using a rotary evaporation, and excess EDA was carefully removed by azeotropic distillation at 35°C using toluene and methanol mixture (9:1) to afford product **G_2** as a yellowish gum (8.15 g, 91%). ^{1}H-NMR (400 MHz, $CDCl_3$): $\delta = 2.22$ (t, $J = 2.3$ Hz, 1H), 2.31–2.38 (m, 12H), 2.52 (t, $J = 6.0$ Hz, 4H), 2.74 (t, $J = 6.0$ Hz, 8H), 2.81 (t, $J = 6.0$ Hz, 12H), 3.22–3.31 (m, 12H), and 3.44 (d, $J = 2.3$ Hz, 2H). MALDI-TOF-MS: Cacld. For $(M + H)^+$ $C_{33}H_{66}N_{13}O_6$: 740.5; found: 740.6.

Boc-protection of PAMAM dendron G_1

A methanol solution (10 mL) of **G_1** (1.08 g, 3.81 mmol) was added slowly into a methanol solution (10 mL) of di-tert-

butyl pyrocarbonate (2.50 g, 11.4 mmol) under −10°C. The solution was stirred for 30 min and then allowed to warm to room temperature. After stirred for 4 h, the mixture was extracted with DCM (50 mL × 3); the combined organic phase was washed with brine (20 mL × 2) and dried over magnesium sulfate. After rotatory evaporation to dryness, repetitive precipitation in hexane afforded Boc-protected G_1 (**G_1-Boc**) as a yellowish solid (1.75 g, 95%). ^{1}H-NMR (400 MHz, $CDCl_3$): $\delta = 1.44$ (s, 18H), 2.22 (t, $J = 2.3$ Hz, 1H), 2.36 (t, $J = 5.9$ Hz, 4H), 2.82 (t, $J = 5.9$ Hz, 4H), 3.23–3.27 (m, 4H), 3.33–3.37 (m, 4H), 3.41 (d, $J = 2.3$ Hz, 2H), and 5.41 (s, 2H).

Synthesis of (4-(azidomethyl)phenyl)methanol 1

A dry DCM solution (20 mL) of thionyl chloride (6.55 g, 55.1 mmol) in a dropping funnel was added dropwise into a dry DCM solution (40 mL) of p-xylylene glycol (6.90 g, 49.9 mmol) at 0°C under nitrogen. The mixture was stirred at 0°C for 1 h and then continued stirring under room temperature for an additional 20 h. The volatiles were removed under reduced pressure, and the residue was then extracted by DCM (50 mL × 3). After rotatory evaporation to dryness, further purification was carried out by flash column chromatography (SiO_2, ethyl acetate/hexane 2:3) to give (4-(chloromethyl)phenyl)methanol (5.15 g, 66%) as a colorless liquid. This compound (4.86 g, 31.0 mmol) dissolved in dry *N*,*N*-dimethylformamide (DMF, 60 mL) was then added dropwise into a DMF suspension of sodium azide (20.3 g, 0.310 mol) under nitrogen. The mixture was then stirred at 80°C overnight. The organic solvent was removed under reduced pressure, and the residue was then extracted by ethyl acetate (50 mL × 2), followed by rotatory evaporation to give **1** as a colorless liquid (3.80 g, 75%). ^{1}H-NMR (400 MHz, $CDCl_3$): $\delta = 2.60$ (s, 1H), 4.30 (s, 2H), 4.62 (s, 2H).7.29 (d, $J = 8.1$ Hz, 2H), and 7.33 (d, $J = 8.1$ Hz, 2H).

Synthesis of bis(4-(azidomethyl)benzyl) malonate 2

A dry DCM solution of dicyclohexylcarbodiimide (DCC, 6.95 g, 33.7 mmol) was added dropwise into a mixed dry DCM/THF (30:10 mL) solution of ***1*** (5.5 g, 33.7 mol), malonic acid (1.59 g, 15.3 mmol), and 1-hydroxybenzotriazole (HOBT, 695 mg, 10 wt % of DCC) under nitrogen at 0°C. After 30 min, the mixture was then stirred under room temperature overnight. The reaction mixture was cooled to 0°C to insure complete precipitation of the byproduct dicyclohexylurea, which is then quickly removed by vacuum filtration. After rotatory evaporation to dryness, further purification was carried out by flash column chromatography (SiO_2, ethyl acetate/hexane 2:3) to give **2** as a colorless liquid (3.50 g, 58%). ^{1}H-NMR (400 MHz, $CDCl_3$): $\delta = 3.49$ (s, 2H), 4.34 (s, 4H), 5.18 (s, 4H), 7.31 (d, $J = 8.2$ Hz, 4H), and 7.34 (d, $J = 8.2$ Hz, 4H).

Synthesis of bis-azido-fullerene derivative 3

A dry toluene (350 mL) solution of C_{60} (350 mg, 0.486 mmol) was added with I_2 (148 mg, 0.583 mmol), **2** (201.3 mg, 0.510 mmol), and 1,8-diazabicycloundec-7-ene (DBU, 155 mg, 1.02 mmol) sequentially. The mixture was stirred under room temperature for 24 h. After rotatory evaporation to dryness, further purification was carried out by flash column chromatography (SiO_2, DCM/hexane 7:3) to give **3** as a brown solid (270 mg, 50%). ^{1}H-NMR (400 MHz, $CDCl_3$): $\delta = 4.36$ (s, 4H), 5.48 (s, 4H), 7.34 (d, $J = 8.4$ Hz, 4H), and 7.44 (d, $J = 8.4$ Hz, 4H).

Synthesis of $C_{60}G_1$ click cluster

A dry THF solution (30 mL) of **G_1-Boc** (246 mg, 0.509 mmol), **3** (270 mg, 0.242 mmol), and CuBr (73.2 mg, 0.510 mmol) was vigorously stirred under room temperature for 3 days and then quenched with aqueous ammonia. The organic solvent was removed using rotatory evaporation, and the residue was then extracted by ethyl acetate (50 mL × 2) to give Boc-protected **$C_{60}G_1$** as a dark brown solid. Carbamate deprotection is readily carried out by acid-promoted hydrolysis. Trifluoroacetic acid (TFA, 611 mg, 5.36 mmol) was added dropwise into a dry DCM solution (15 mL) of Boc-protected **$C_{60}G_1$** (226 mg, 0.109 mmol). The mixture was then stirred under room temperature for 2 days, and the volatiles were removed under reduced pressure. The mixture was washed with hexane repetitively to remove excess acid, and then freeze-drying afforded **$C_{60}G_1$** as a brown fluffy powder (207 mg, 89%). ^{1}H-NMR (400 MHz, $CDCl_3$): $\delta = 2.82$ (t, $J = 6.4$ Hz, 8H), 3.09 (t, $J = 6.4$ Hz, 8H), 3.47 (t, $J = 6.4$ Hz, 8H), 3.56 (t,$J = 6.4$ Hz, 8H), 4.14 (d, $J = 2.0$ Hz, 4H), and 7.87 (s, 2H). MALDI-TOF-MS: Cacld. For $(M + H)^+$ $C_{105}H_{66}N_{16}O_8$: 1679.75; found: 1680.46. Cacld. For $(M + Na)^+$ $C_{105}H_{66}N_{16}NaO_8$: 1702.74; found: 1702.53.

Ethidium bromide displacement assay

0.5 mL of pEGFP-C1 solution (1 μg mL^{-1}) and 7 μL of ethidium bromide (EtBr) solution (0.1 mg mL^{-1}) were mixed thoroughly in vials, followed by adding 8 μL of $C_{60}G_1$ solutions to achieve the desired N/P = 0.6, 0.8, 1.0, 1.2, and 2.0. Aliquots (200 μL) of thus-prepared solutions were then added into each well of 96-well black plates for the fluorescence measurement. 7 μL of EtBr (0.1 mg mL^{-1}) in ultrapure water (508 μL) was measured as the background fluorescence of EtBr, and the solution that only contains pEGFP-C1 and EtBr in 1:1 binding ratio corresponds to the N/P = 0 with maximum emission intensity. The fluorescence measurement was performed on Molecular Devices FlexStation 3 microplate reader using an excitation wavelength of 260 nm, and the emission spectra were recorded from 540 nm to 700 nm.

Characterization of complex morphology, size, and ζ-potential

For atomic force microscopic analysis, 5 μL of each sample was placed on a freshly cleaved mica sheet. After 5 min incubation at room temperature, the sheet was washed twice with 100 μL of double-distilled H_2O. The prepared samples were first dried from the edge of the mica sheet using a paper tissue, then by exposure to gentle air flow for 10 min. The samples were then immediately subjected to AFM study. We used a Nanoscope IIIa Multimode scanning probe microscope from Digital Instruments (Veeco Metrology Group,

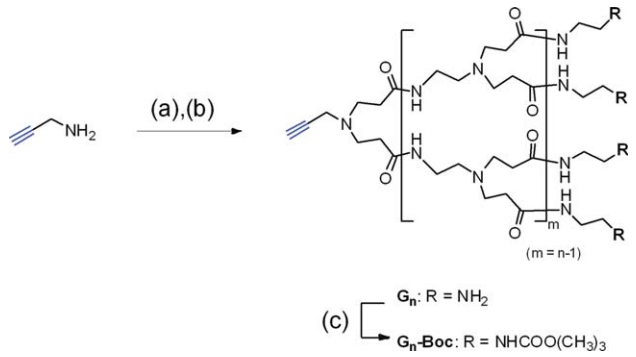

FIGURE 1. Synthesis of $\mathbf{G_1}$ and $\mathbf{G_2}$ PAMAM dendrons bearing a propargyl focal point. (a) methyl acrylate, methanol; (b) EDA, methanol; and (c) di-tert-butyl pyrocarbonate, methanol. [Color figure can be viewed in the online issue, which is available at wileyonlinelibrary.com.]

Santa Barbara, CA) in contacting mode with scan rate of 2.441 Hz and tip velocity of 2.35 μm s^{-1}. Analyses of the images were carried out using the Nanoscope III software version 5.31R1. Dynamic light scattering (DLS) and ζ-potential measurements were performed on Malvern Zetasizer Nano series. Transmission electron microscopy (TEM) images were taken by a Hitachi H-7000 electron microscope with Hamamatsu C4742-95 digital camera operated at an accelerating voltage of 100 kV.

Cellular uptake of the $C_{60}G_1$/DNA complexes

HeLa cells and MCF-7 cells were obtained from the American Type Culture Collection (ATCC, Manassas, VA). MCF-7 cells were cultured in MEMα medium (Life Technologies Corporation) supplemented with 10% fetal bovine serum (Hyclone), bovine insulin (5 μg mL^{-1}, Sigma-Aldrich), sodium pyruvate (1 m*M*; Biological Industries), antibiotics (100 U mL^{-1} penicillin and 100 μg mL^{-1} streptomycin; Life Technologies Corporation), and Glutamax (2 m*M*; Life Technologies Corporation). HeLa cells were cultured in DMEM medium (Life Technologies Corporation) with supplements as used for MCF-7 cultivation except for bovine insulin. The cells were maintained in a 5% CO_2 air humidified atmosphere at 37°C.

To evaluate the cellular uptake efficiency of the $C_{60}G_1$/DNA complex, pEGFP-C1 (Clontech) was labeled with YOYO-1 fluorescent dye (Life Technologies Corporation). Briefly, 500 μL of pEGFP-C1 solution in water (1 μg mL^{-1}) was mixed with 4 μL of 200 μ*M* YOYO-1 and incubated at room temperature for 10 min. Then, 3.2 μL of $C_{60}G_1$ (0.5 μg μL^{-1}) and TurboFect (Fermentas, Thermo Scientific, Pittsburgh, PA) containing YOYO-1-labeled plasmid DNA were added to the cells with the complete medium (DMEM with 10 % FBS and antibiotics), and further cultured for 2 h before being harvested for fluorescence microscope and flow cytometric analysis.

Fluorescence microscopy and flow cytometry

For observation of GFP+ cells, cells were observed for green fluorescence signals with inverted fluorescent microcopy (Axioskop 2, ZEISS, Germany) with 100 W halogen lamp, 480/30 nm band-pass blue excitation filter, a 505 nm dichroic mirror, and a 535/40 nm band-pass barrier filter. Images were captured with cool CCD camera and processed with MetaMorph Software (Molecular Devices). For quantification with GFP+ cells, cells were harvested with trypsin/EDTA, resuspended in 200 μL of PBS/1 % bovine serum albumin (Sigma-Aldrich), and analyzed by flow cytometry (Epics XL, Beckman Coulter). The green fluorescence emission (525 nm) illuminated with 488nm blue laser and signals were collected with software provided by the manufacture. The percentage and mean fluorescence intensity of GFP+ cells were further analyzed by WinMDI software (The Scripps Research Institute, San Diego). Each data shown in Figure 9 was expressed as mean ± standard deviation of three experiments.

Agarose gel electrophoresis analysis of complexing capacity between $C_{60}G_1$ and DNA

0.5 μg of pEGFP-C1 palsmid DNA was dissolved in nuclease-free H_2O and $C_{60}G_1$ was then added at different N/P ratio (range from 0.5 to 2.0) to final volume of 15 μL. After mixing well and incubating at room temperature for 30 min, the $C_{60}G_1$/DNA solutions were added with 3 μL of Novel juice DNA loading dye (GeneDirex), loaded into wells of 1.0 % agarose gel, and performed electrophoresis in TAE buffer (40 m*M* Tris-acetate, 1 m*M* Na_2-EDTA, pH = 8.5) at 150 V for 1 h. DNA signals were detected by SafeBlue Imager System (Major Science, Saratoga, CA) with a blue light LED source to visualize the DNA bands and images were captured by a digital camera (Canon G15; Ohta-ku, Tokyo, Japan). The intensities of DNA bands were analyzed by ImageJ software (NIH, Bethesda. MA).

RESULTS AND DISCUSSION

Material synthesis and characterization

Our strategy for the synthesis of amphiphilic C_{60}-PAMAM-dendron click clusters comprised 2 parts. (1) The preparation of a counterpart: the NH_2-terminated PAMAM dendron

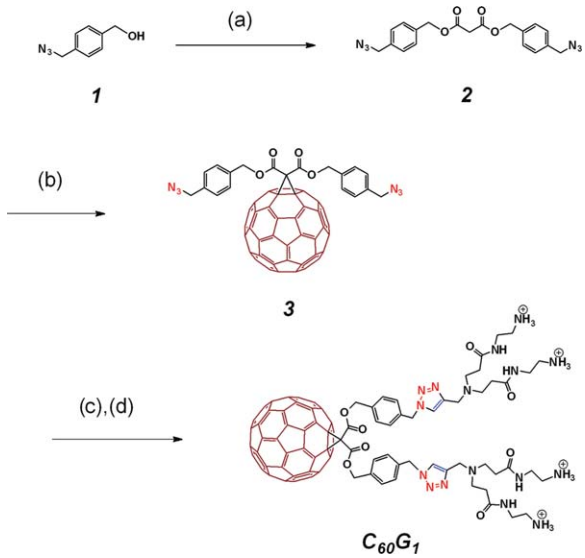

FIGURE 2. Synthesis of amphiphilic PAMAM dendron-bearing C_{60} click cluster ($\mathbf{C_{60}G_1}$). (a) malonic acid, DCC, HOBT, THF/CH_2Cl_2, 0°C to room temperature; (b) C_{60}, DBU, I_2, toluene; (c) $\mathbf{G_1}$-**Boc**, CuBr, THF; and (d) TFA, CH_2Cl_2. [Color figure can be viewed in the online issue, which is available at wileyonlinelibrary.com.]

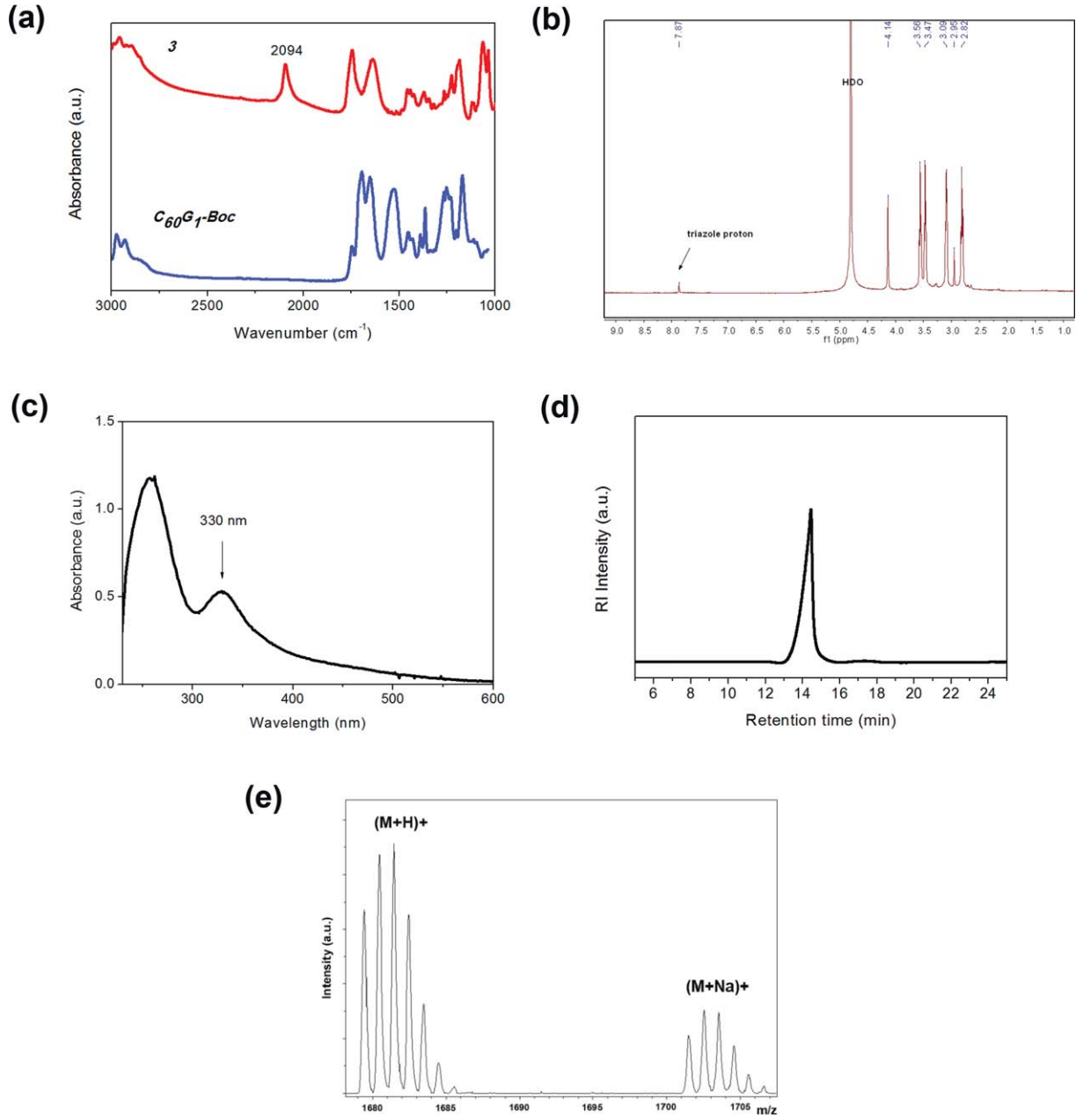

FIGURE 3. (a) FT-IR spectra of **3** and Boc-protected $\mathbf{C_{60}G_1}$. (b) ^{1}H-NMR spectrum, (c) UV–Vis spectrum, (d) GPC chromatogram, and (e) MALDI-TOF-MS spectrum of $\mathbf{C_{60}G_1}$. [Color figure can be viewed in the online issue, which is available at wileyonlinelibrary.com.]

was prepared by a divergent pathway using propargylamine as the focal point. As shown in Figure 1, a conventional 2-step procedure consisting of a Michael addition followed by amidation produces the G_1 PAMAM dendron. All NH_2 terminals were then protected with Boc groups to prevent unwanted complexation with the copper catalysts; (2) as shown in Figure 2, the diazido-functionalized fullerene derivative was prepared in high yield by a Bingel reaction. The conjugation of the as-prepared PAMAM dendrons and the C_{60} derivative was conducted through a CuAAC ("click" reaction) to produce the protected click clusters. Finally, acidic hydrolysis was performed to deprotect the amino groups, and produce the highly water-soluble amphiphilic C_{60} and G_1 PAMAM dendron conjugate, namely $C_{60}G_1$.

$C_{60}G_1$ and its precursors were fully characterized by ^{1}H-NMR, FT-IR, UV–Vis spectroscopy, GPC, and MALDI-TOF mass spectrometry. The ^{1}H- and ^{13}C-NMR spectra of compounds **2** and **3** (Supporting Information Figs. S1 and S2) clearly indicate the successful synthesis of a Bingel adduct with diazido groups, by the disappearance of the malonate center protons at 3.5 ppm. Notably, although the azido group could attack the fullerene moiety to cause cycloaddition, compound **2** was stable in dilute solution. FT-IR spectroscopy confirmed the success of the click coupling

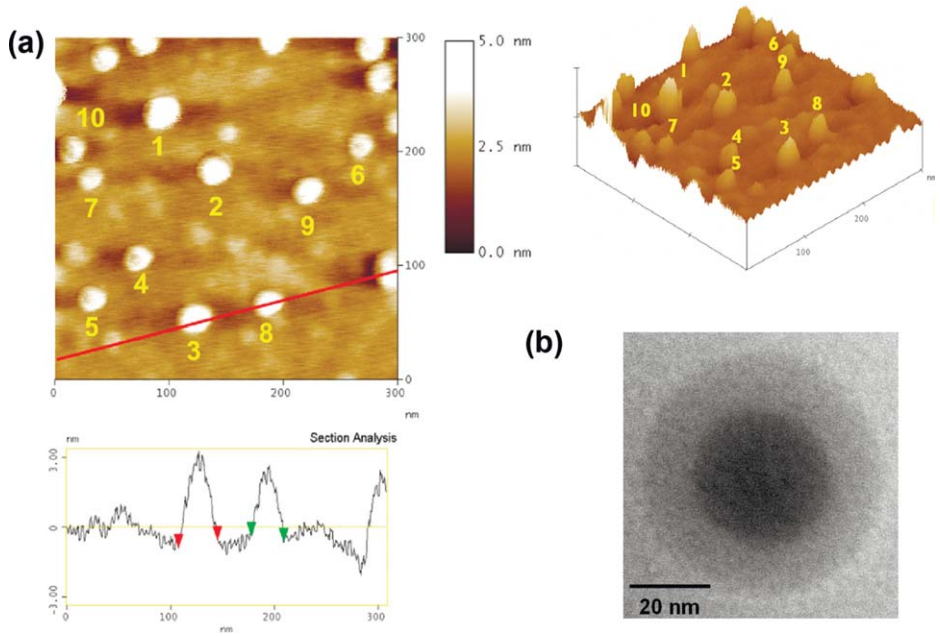

FIGURE 4. (a) Atomic force micrograph and section analysis for $\mathbf{C_{60}G_1}$ aggregates on mica surface. The particle dimension averaged by 10 selected particles is 22.4 ± 3.7 nm. (b) Transmission electron micrograph of core–shell-like $\mathbf{C_{60}G_1}$ aggregates. [Color figure can be viewed in the online issue, which is available at wileyonlinelibrary.com.]

between the Boc-protected G_1 PAMAM dendron and the diazido fullerene, by the disappearance of the azide stretching band at 2094 cm^{-1} [Fig. 3(a)], and by the appearance of characteristic proton and carbon resonances of the click counterpart in the ^{1}H-NMR spectra (Supporting Information Fig. S3). Finally, complete deprotection of the Boc groups was confirmed by the disappearance of the corresponding protons at 1.5 ppm from the ^{1}H-NMR spectrum, supporting the formation of the highly water-soluble cationic C_{60} derivative bearing two NH_2-terminated G_1 PAMAM dendrons [Fig. 3(b)]. Additionally, the appearance of the triazole proton resonance at 7.9 ppm suggests that CuAAC click coupling was successful, indicating the exclusive formation of the 1,4-regioisomer.[32] Moreover, UV–Vis analysis of the as-prepared click clusters [Fig. 3(c)] show a broad absorption maximum at approximately 330 nm, clearly indicating the existence of a fullerene core. Aqueous phase GPC combined with cationic exchange chromatography [Fig. 3(d)] revealed monodispersed elution peaks for $C_{60}G_1$, confirming that the click reaction produced a single product in high purity. MALDI-TOF mass spectrometry results support our proposed structure by demonstrating an exact match between calculated and observed molar masses for the $C_{60}G_1$ click cluster [Fig. 3(e)].

Self-aggregation of amphiphilic $C_{60}G_1$ and DNA complexes

Because of its amphiphilic nature, $C_{60}G_1$ assembles into core–shell-like micelles rather than remaining in a single molecular form in aqueous media.[33] Therefore, we used AFM to analyze the $C_{60}G_1$self-aggregation behavior. Figure 4(a) shows microscopic images of $C_{60}G_1$ deposited on a freshly cleaved mica surface, clearly confirming the formation of nanoclusters, with an average dimension of 22.4 ± 3.7 nm. The results of DLS experiments were in agreement with the AFM results, indicating comparable dimensions for these micelle-like nanoparticles, with a *z*-average size distribution of 24.8 ± 0.2 nm, and a polydispersity index of 0.255 ± 0.008. Both sets of data are consistent with the magnitude of primary micelles comprising a hydrophobic C_{60} core and hydrophilic PAMAM dendron shell. Moreover, TEM analysis demonstrated a micelle-like structure with sharp contrast between the core and shell components [Fig. 4(b)].

Recently, López et al.[34] reported a series of regioisomeric dendron-fulleropyrrolidines with no aggregation occurring up to 10^{-3} mol L^{-1}. However, on the basis of AFM and DLS analysis, we found that the $C_{60}G_1$ favors the formation of nanoparticles at much lower concentration of approximately 5×10^{-6} mol L^{-1}. Thus, C_{60} could serve as a hydrophobic building block, and so drive PAMAM dendron assembly to form a "pseudodendrimer." Moreover, zeta-potential measurement further indicated that these C_{60}-centered pseudodendrimers carry multiple positive charges on their surfaces (22.3 ± 5.2 mV), allowing electrostatic interactions with polyanionic targets such as plasmid DNA.

We evaluated the binding affinity of amphiphilic $C_{60}G_1$ toward pEGFP-C1 (4731 base pairs) using an EtBr displacement assay.[35] The DNA intercalating agent EtBr is commonly used in molecular biology to detect nucleic acids. The competition for binding with DNA, between EtBr reagents and polyamine-based vectors toward DNA, allows us to determine the minimum N/P ratio necessary for effective complexation. In the assay, the optimized N/P ratio is

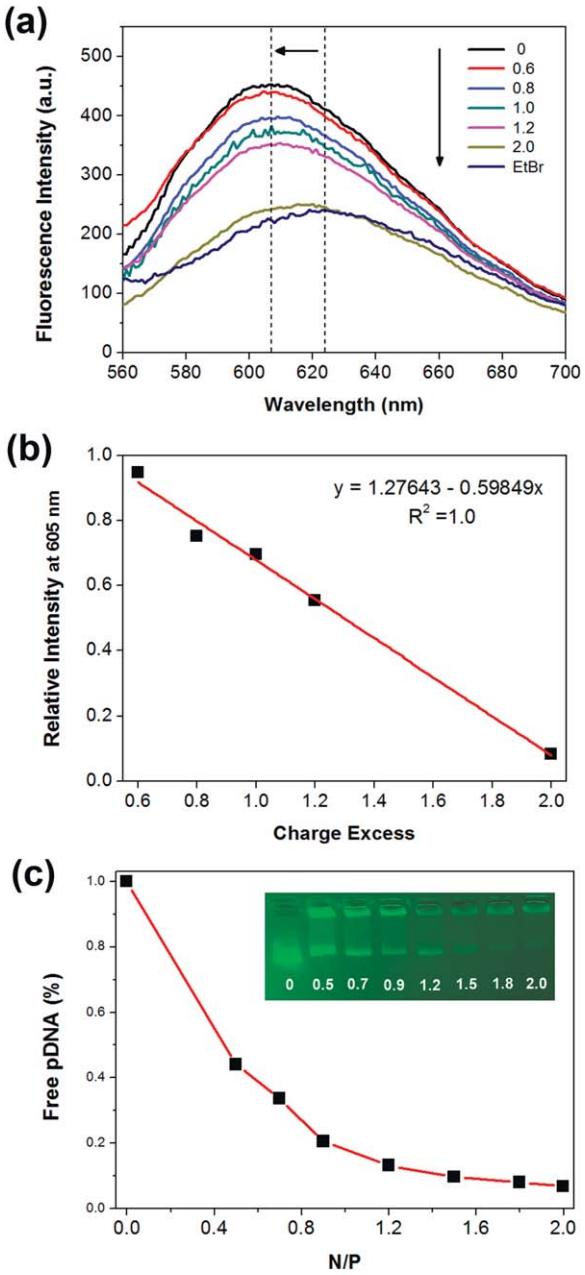

FIGURE 5. (a) Fluorescence titration data for the addition of $\mathbf{C_{60}G_1}$ to DNA at various nitrogen-to-phosphorous (N/P) ratios. The maximum fluorescence intensity corresponds to the 1:1 binding of EtBr and a DNA base in the absence of $\mathbf{C_{60}G_1}$, and the minimum intensity corresponds to the amount of free EtBr in water. (b) The linear correlation of relative fluorescence intensities at 605 nm versus the charge excess values. (c) Agarose gel electrophoresis analysis for determining the optimized binding capacity of $\mathbf{C_{60}G_1}$ at various N/P ratios. [Color figure can be viewed in the online issue, which is available at wileyonlinelibrary.com.]

expressed as a 50% charge excess (CE_{50}) value, which represents the "excess charge" on the cationic vector relative to anionic DNA that is required for 50% EtBr displacement. A lower CE_{50} value, provided by a smaller N/P ratio, represents more effective binding of the 2 components. Figure 5(a) provides fluorescence titration data for the addition of $C_{60}G_1$, where the maximum fluorescence intensity corresponds to the 1:1 binding of EtBr and a DNA base in the absence of $C_{60}G_1$, and the minimum intensity corresponds to the amount of free EtBr in water. We attributed the enhanced and blue-shifted emission pattern arising from the intercalating complex to the less polar environment inside the DNA helix. Emission intensity continually decreased with increasing $C_{60}G_1$ concentration, suggesting that intercalating EtBr molecules were gradually displaced by C_{60}-based

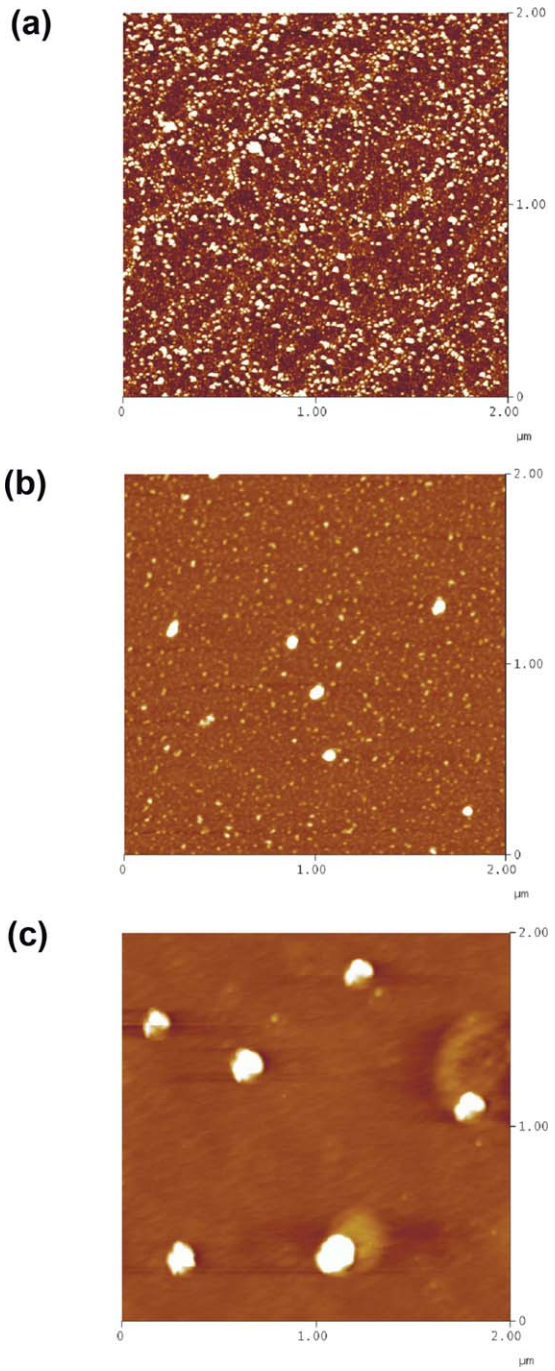

FIGURE 6. Atomic force micrographs of initial $\mathbf{C_{60}G_1}$ (4.7×10^{-6} mol L^{-1}) on 2 × 2 µm mica surface (a), mixing DNA with $\mathbf{C_{60}G_1}$ at N/P = 2 for 30 min (b), and 180 min (c). [Color figure can be viewed in the online issue, which is available at wileyonlinelibrary.com.]

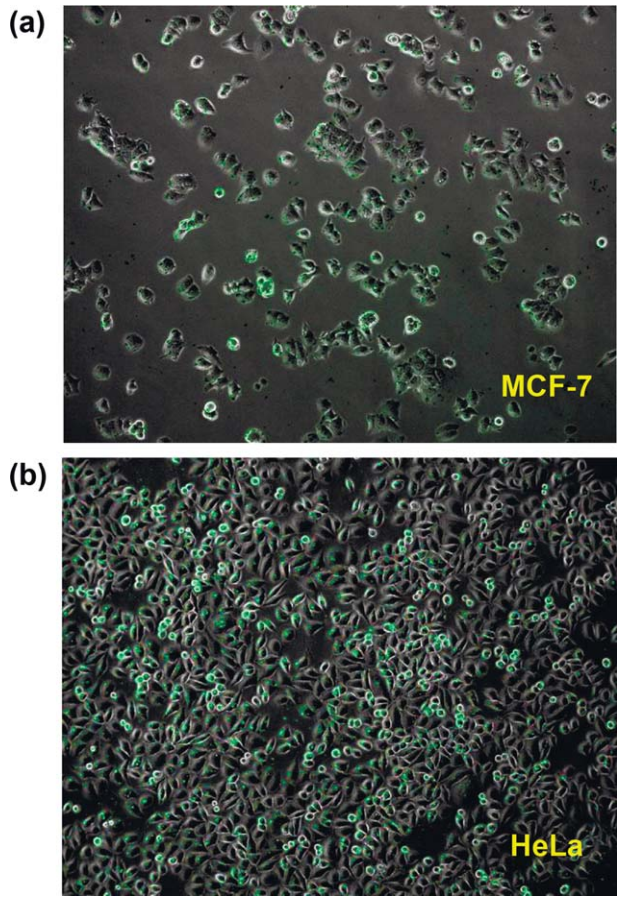

FIGURE 7. The overlaying optical and fluorescence microscope images for (a) MCF-7 and (b) HeLa cell lines internalized by **$C_{60}G_1$**/DNA complexes at N/P = 2. The green spots represent a successful cellular uptake of YOYO-1-labeled DNA. [Color figure can be viewed in the online issue, which is available at wileyonlinelibrary.com.]

vectors. The CE_{50} value calculated from the linear correlation of relative fluorescence intensities at 605 nm versus the CE values was found to be only 1.3 [Fig. 5(b)], clearly confirming that amphiphilic $C_{60}G_1$ is an effective DNA binder. Barnard et al.[36] demonstrated the effective DNA binding of a family of amphiphilic dendrons bearing either long alkyl chains or cholesterols as the hydrophobic building blocks. The authors reported that self-assembled dendrons consistently achieved superior EtBr displacement, and had lower CE_{50} values, compared to non-self-assembled complexes. In our study, we found that a net positive charge of +4 per $C_{60}G_1$ molecule was insufficient to displace more than 50% of EtBr from its intercalation sites. However, the strong interaction of the hydrophobic C_{60} moiety is capable of inducing the close-packing of positively charged dendrons to form a C_{60}-based pseudodendrimer, by which DNA could be more efficiently wrapped into compact electrostatic complexes of a size that is suitable for cellular uptake. Additionally, gel electrophoresis analysis confirmed strong binding between $C_{60}G_1$ and DNA; more than 90% of DNA bound to C_{60}-based vectors at N/P ratios greater than 1.2 [Fig. 5(c)], consistent with our spectroscopic results.

AFM scanning was used to further visualize the morphology of the $C_{60}G_1$ and DNA complex at an optimized ratio of N/P = 2 to ensure complete binding between the vector and nucleic acids. Figure 6 shows micrographs of the as-formed complexes on a 2 × 2 μm mica surface, confirming the electrostatic condensation of $C_{60}G_1$ with DNA, and clearly indicating a dynamic formation process. The small white dots in Figure 6(a) represent uniformly dispersed $C_{60}G_1$ nanoclusters; Figure 6(b) shows their partial aggregation into larger particles 30 min after mixing with pEGFP-C1 in water. At this stage, free $C_{60}G_1$ self-aggregates predominated over the DNA complexes, however, after standing for 3 h, the mixing solution exclusively contained the electrostatic DNA complexes, with an average diameter of approximately 140 nm, as determined by AFM section analysis [Fig. 6(c)]. DLS measurements also verified the dynamic formation process by revealing an increasing particle size distribution and narrowing polydispersity index, from 93 nm and 0.37, to 110 nm and 0.29, respectively. An optimized N/P ratio is a critical factor in DNA complex formation using polyamine-based vectors. Both AFM and DLS analyses suggested that extended complexation time benefit the formation of DNA/$C_{60}G_1$ hybrid nanoparticles with favorable dimensions for cellular uptake.

Gene delivery into HeLa and MCF-7 cell lines

We performed a cellular uptake study using fluorescent YOYO-1 cyanine-based probes, which readily intercalate DNA with high binding affinity.[37] YOYO-1 does not emit fluorescence until bound to double-stranded DNA, when the emission intensity for these complexes dramatically

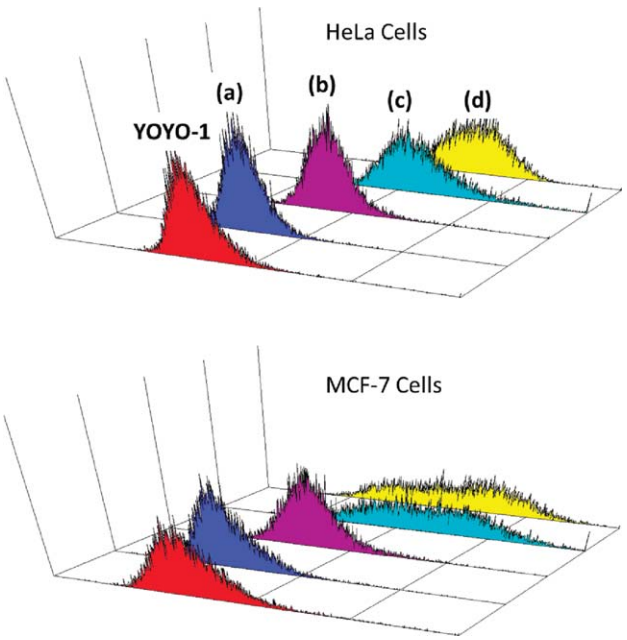

FIGURE 8. The flow cytometry histograms for counting 1×10^{-4} cells internalized by (a) DNA/YOYO-1, (b) **$C_{60}G_1$**/YOYO-1, (c) TurboFect/DNA/YOYO-1, and (d) **$C_{60}G_1$**/DNA/YOYO-1 complexes at N/P = 2. The incident laser wavelength was set to 488 nm. [Color figure can be viewed in the online issue, which is available at wileyonlinelibrary.com.]

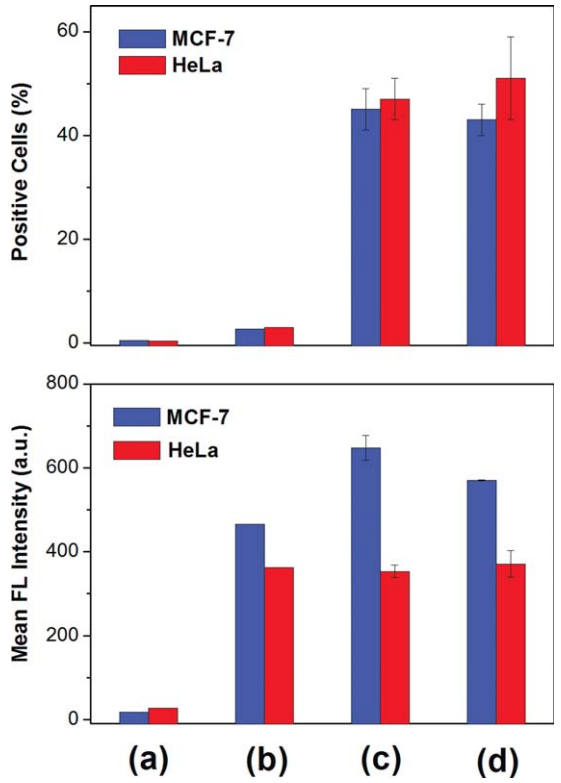

FIGURE 9. The quantitative analysis for flow cytometry in terms of positive cells and mean fluorescence intensity for cells internalized by (a) DNA/YOYO-1, (b) **$C_{60}G_1$**/YOYO-1, (c) TurboFect/DNA/YOYO-1, and (d) **$C_{60}G_1$**/DNA/YOYO-1 complexes at N/P = 2,, where the concentrations of **$C_{60}G_1$**, DNA bases, and YOYO-1 are 1.51, 3.03, and 1.60 $\times$ 10^{-6} mol L^{-1}, respectively. [Color figure can be viewed in the online issue, which is available at wileyonlinelibrary.com.]

increases (Supporting Information Fig. S4). The fluorescence enhancement observed during the cellular uptake experiment confirmed the uptake of YOYO-1 labeled DNA, and allowed us to trace the *in vitro* and *in vivo* biodistributions of nucleic acids. To evaluate $C_{60}G_1$-mediated gene delivery, pEGFP-C1 was pretreated with YOYO-1, followed by mixing with $C_{60}G_1$ at an N/P ratio of 2, to ensure complete association between DNA, vectors, and probe molecules. A commercially available transfection reagent (TurboFect) was used as a positive control for two cell lines—a breast cancer cell line, MCF-7 and a cervical cancer cell line, HeLa. Fluorescent microscopic images clearly show that the $C_{60}G_1$/DNA complexes are taken up by both MCF-7 and HeLa cells (Fig. 7).

Flow cytometry analysis was performed to quantify the MCF-7 and HeLa cellular uptake efficiencies of $C_{60}G_1$/DNA. Because the self-penetrating behavior of fluorescence dyes may affect the counting of positive cells, we used cells transfected by YOYO-1 alone as the negative control for the flow cytometry analysis. Notably, the result revealed YOYO-1 self-penetration into the target cell lines without the aid of a vector; and approximately 59% of HeLa cells were YOYO-1 positive, with weak mean fluorescence intensity of 48 units (Supporting Information Fig. S5). The flow histograms shown in Figure 8 indicate that the complex could be taken up by both MCF-7 and HeLa cells, in agreement with the microscopic results. Figure 9 lists quantitative data in terms of the positive cells, and the mean fluorescence intensities for cells transfected by YOYO-1, DNA/YOYO-1 [Fig. 9(a)], $C_{60}G_1$/YOYO-1 [Fig. 9(b)], TurboFect/DNA/YOYO-1 [Fig. 9(c)], and $C_{60}G_1$/DNA/YOYO-1 complexes [Fig. 9(d)]. Comparing the two cell lines, we found that at an N/P ratio of 2, the overall uptake efficiency of $C_{60}G_1$/DNA complexes toward HeLa cells was slightly greater than that for MCF-7 cells. Approximately 51% of HeLa cells were internalized by the $C_{60}G_1$/DNA complexes, where the mean fluorescence intensity was 371 units, and approximately 43% of MCF-7 cells were positive to the complexes, with a mean fluorescence intensity of 570 units. These results suggest that using $C_{60}G_1$ assembly as a DNA vehicle is comparable to the TurboFect–mediated delivery system. We also performed a control experiment using amine-terminated G_2 PAMAM Dendron as the gene vector, and no cellular uptake was observed at the N/P value of 2 (Supporting Information Fig. S6). The G_2 dendron bears the same number of surface charges as $C_{60}G_1$, but lacks sufficient self-aggregation to deliver DNA into the target cells. Thus, the amphiphilic structure of $C_{60}G_1$ is crucial for gene delivery. Moreover, while comparing Figure 9(a,b), we found that approximately 3% of cells were internalized by YOYO-1 with remarkable fluorescence enhancement in the presence $C_{60}G_1$ (465 units for MCF-7 cells and 362 units for HeLa cells). Although the mechanism is unclear, we speculated that $C_{60}G_1$ is also capable of delivering rigid aromatic compounds into target cells.

CONCLUSION

Using a "pseudodendrimer" composed of amphiphilic dendrons as a nonviral gene vector, we developed a simple synthesis for a NH_2-terminated PAMAM dendron-bearing fullerenyl dyad through the CuAAC click reaction. The amphiphilic structure and solvophobic nature of C_{60} induce the dyad to form uniform core–shell-like nanoparticles in water. The polycationic C_{60}-based nanoparticles bind firmly with negatively charged pDNA at low N/P ratios, and both HeLa and MCF-7 cell lines readily take up the resulting electrostatic complexes. On the basis of the favorable binding affinity and cellular uptake obtained using C_{60}-based nanoparticles as carrier, investigations along gene transfection and EGFP expression are now underway and will be reported in due course.

ACKNOWLEDGMENTS

NMR analysis was performed in the Instrument Center of Chung Shan Medical University, which is supported by the National Science Council, Ministry of Education, and Chung Shan Medical University.

REFERENCES

1. Tang MX, Redemann CT, Szoka FC. In vitro gene delivery by degraded polyamidoamine dendrimers. Bioconjugate Chem 1996; 7:703–714.

2. Navarro G, Tros de Ilarduya C. Activated and non-activated PAMAM dendrimers for gene delivery in vitro and in vivo. Nanomedicine 2009;5:287–297.
3. Yellepeddi VK, Kumar A, Palakurthi S. Biotinylated poly(amido amine) (PAMAM) dendrimers as carriers for drug delivery to ovarian cancer cells in vitro. Anticancer Res 2009;29:2933–2943.
4. Esfand R, Tomalia DA. Poly(amido amine) (PAMAM) dendrimers: From biomimicry to drug delivery and biomedical applications. Drug Discov Today 2001;6:427–436.
5. Menjoge AR, Kannan RM, Tomalia DA. Dendrimer-based drug and imaging conjugates: Design considerations for nanomedical applications. Drug Discov Today 2010;15:171–185.
6. Tomalia DA. Dendrons/dendrimers: Quantized, nano-element like building blocks for soft–soft and soft–hard nano-compound synthesis. Soft Matter 2010;6:456–474.
7. Rosen BM, Wilson CJ, Wilson DA, Peterca M, Imam MR, Percec V. Dendron-mediated self-assembly, disassembly, and self-organization of complex systems. Chem Rev 2009;109:6275–6540.
8. Russ V, Elfberg H, Thoma C, Kloeckner J, Ogris M, Wagner E. Novel degradable oligoethylenimine acrylate ester-based pseudodendrimers for in vitro and in vivo gene transfer. Gene Ther 2008; 15:18–29.
9. Santos JL, Oliveira H, Pandita D, Rodrigues J, Pêgo AP, Granja PL, Tomás H. Functionalization of poly(amido amine) dendrimers with hydrophobic chains for improved gene delivery in mesenchymal stem cells. J Controlled Release 2010;144:55–64.
10. Yuba E, Nakajima Y, Tsukamoto K, Iwashita S, Kojima C, Harada A, Kono K. Effect of unsaturated alkyl chains on transfection activity of poly(amido amine) dendron-bearing lipids. J Controlled Release 2012;160:552–560.
11. Yu T, Liu X, Bolcato-Bellemin AL, Wang Y, Liu C, Erbacher P, Qu F, Rocchi P, Behr JP, Peng L. An amphiphilic dendrimer for effective delivery of small interfering RNA and gene silencing in vitro and in vivo. Angew Chem Int Ed 2012;51:8478–8484.
12. Guillot-Nieckowski M, Joester D, Stöhr M, Losson M, Adrian M, Wagner B, Kansy M, Heinzelmann H, Pugin R, Diederich F, Gallani JL. Self-assembly, DNA complexation, and pH response of amphiphilic dendrimers for gene transfection. Langmuir 2006; 23:737–746.
13. Takahashi T, Kono K, Itoh T, Emi N, Takagishi T. Synthesis of novel cationic lipids having polyamidoamine dendrons and their transfection activity. Bioconjugate Chem 2003;14:764–773.
14. Guillot M, Eisler S, Weller K, Merkle HP, Gallani JL, Diederich F. Effects of structural modification on gene transfection and self-assembling properties of amphiphilic dendrimers. Org Biomol Chem 2006;4:766–769.
15. Bakry R, Vallant RM, Najam-ul-Haq M, Rainer M, Szabo Z, Huck CW, Bonn GK. Medicinal applications of fullerenes. Int J Nanomed 2007; 2: 639–649.
16. Cha C, Shin SR, Annabi N, Dokemci MR, Khademhosseini A. Carbon-based nanomaterials: Multifunctional materials for biomedical engineering. ACS Nano 2013;7:2891–2897.
17. Chen ML, He YJ, Chen XW, Wang JH. Quantum-dot-conjugate graphene as a probe for simultaneous cancer-targeted fluorescence imaging, tracking, and monitoring drug delivery. Bioconjugate Chem 2013;24:387–397.
18. Shen H, Zhang L, Liu M, Zhang, Z. Biomedical applications of graphene. Theranostics 2012;2:283–294.
19. Liu JH, Cao L, Luo PG, Yang ST, Lu F, Wang H, Meziani MJ, Haque SA, Liu Y, Lacher S, Sun YP. Fullerene-conjugated doxorubicin in cells. ACS Appl Mater Interfaces 2010;5:1384–1389.
20. Mamiya R, Noiri E, Isobe H, Nakanishi W, Okamoto K, Doi K, Sugaya T, Izumi T, Homma T, Nakamura E. In vivo gene delivery by cationic tetraamino fullerene. PNAS 2010;107:5339–5344.
21. Isobe H, Nakanishi W, Tomita N, Jinno S, Okayama H, Nakamura E. Gene delivery by aminofullerenes: Structural requirements for efficient transfection. Chem-Asian J 2006;1:167–175.
22. Isobe H, Sugiyama S, Fukui K, Iwasawa Y, Nakamura E. Atomic force microscope studies on condensation of plasmid DNA with functionalized fullerenes. Angew Chem Int Ed 2001;40:3364–3367.
23. Isobe H, Nakanishi W, Tomita N, Jinno S, Okayama H, Nakamura, E. Nonviral gene delivery by tetraamino fullerene. Mol Pharm 2005;3:124–134.
24. Brettreich M, Burghardt S, Böttcher C, Bayerl T, Bayerl S, Hirsch A. Globular amphiphiles: Membrane-forming hexaadducts of C_{60}. Angew Chem Int Ed 2000;39:1845–1848.
25. Zhou S, Burger C, Chu B, Sawamura M, Nagahama N, Toganoh M, Hackler UE, Isobe H, Nakamura E. Spherical bilayer vesicles of fullerene-based surfactants in water: a laser light scattering study. Science 2001;291:1944–1947.
26. Burger C, Hao J, Ying Q, Isobe H, Sawamura M, Nakamura E, Chu B. Multilayer vesicles and vesicle clusters formed by the fullerene-based surfactant $C_{60}(CH_3)_5K$. J Colloid Interface Sci 2004; 275:632–641.
27. Joester D, Losson M, Pugin R, Heinzelmann H, Walter E, Merkle HP, Diederich F. Amphiphilic dendrimers:novel self-assembling vectors for efficient gene delivery. Angew Chem Int Ed 2003;42:1486–1490.
28. Jones SP, Gabrielson NP, Pack DW, Smith DK. Synergistic effects in gene delivery—a structure–activity approach to the optimisation of hybrid dendritic–lipidic transfection agents. Chem Commun 2008:4700–4702.
29. Posocco P, Pricl S, Jones S, Barnard A, Smith DK. Less is more—multiscale modelling of self-assembling multivalency and its impact on DNA binding and gene delivery. Chem Sci 2010;1:393–404.
30. Jones SP, Gabrielson NP, Wong CH, Chow HF, Pack DW, Posocco P, Fermeqlia M, Pricl S, Smith DK. Hydrophobically modified dendrons: developing structure-activity relationships for DNA binding and gene transfection. Mol Pharm 2011;8:416–429.
31. Meldal M, Tornøe CW. Cu-catalyzed azide-alkyne cycloaddition. Chem Rev 2008;108:2952–3015.
32. Srinivasachari S, Fichter KM, Reineke TM. Polycationic β-cyclodextrin "click clusters": Monodisperse and versatile scaffolds for nucleic acid delivery. J Am Chem Soc 2008;130:4618–4627.
33. Chu CC, Tsai YJ, Hsiao LC, Wang LY. Controlled self-aggregation of C_{60}-anchored multiarmed polyacrylic acids and their cytotoxicity evaluation. Macromolecules 2011;44:7056–7061.
34. López AM, Scarel F, Carrero NR, Vázquez E, Mateo-Alonso A, Da Ros T, Prato M. Synthesis and characterization of highly water-soluble dendrofulleropyrrolidine bisadducts with DNA binding activity. Org Lett 2012;14:4450–4453.
35. Geall AJ, Blagbrough IS. Rapid and sensitive ethidium bromide fluorescence quenching assay of polyamine conjugate–DNA interactions for the analysis of lipoplex formation in gene therapy. J Pharm Biomed Anal 2000;22:849–859.
36. Barnard A, Posocco P, Pricl S, Calderon M, Haag R, Hwang ME, Shum VW, Pack DW, Smith DK. Degradable self-assembling dendrons for gene delivery: experimental and theoretical insights into the barriers to cellular uptake. J Am ChemSoc 2011;133: 20288–20300.
37. Becker B, Clapper J, Harkins KR, Olson JA. In situ screening assay for cell viability using a dimeric cyanine nucleic acid stain. Anal Biochem 1994;221:78–84.